BNL-207922-2018-JAAM

Comparison of soil organic carbon speciation using C NEXAFS and CPMAS C-13 NMR spectroscopy

J. Prietzel, J. Thieme

To be published in "SCIENCE OF THE TOTAL ENVIRONMENT"

July 2018

Photon Sciences

Brookhaven National Laboratory

U.S. Department of Energy

USDOE Office of Science (SC), Basic Energy Sciences (BES) (SC-22)

DISCLAIMER

Comparison of soil organic carbon speciation using C NEXAFS and CPMAS ^{13}C NMR spectroscopy

Jörg Prietzel [a,*], Svenja Müller [a], Ingrid Kögel-Knabner [a], Jürgen Thieme [b], Cherno Jaye [c], Daniel Fischer [c]

[a] Chair of Soil Science, Dept. of Ecology and Ecosystem Management, Munich University of Technology, Emil-Ramann-Str. 2, 85354 Freising, Germany
[b] NSLS II, Brookhaven National Laboratory, Upton, NY, USA
[c] Material Measurement Laboratory, National Institute of Standards and Technology, Gaithersburg, MD 20899, USA

HIGHLIGHTS

- Comparison of soil carbon speciation using C NEXAFS and CPMAS ^{13}C NMR spectroscopy
- Analysis of defined mixtures of SOM sources, organic layer, mineral soil samples
- CPMAS ^{13}C NMR more accurate and precise than C NEXAFS spectroscopy
- C NEXAFS spectroscopy excellent method for analysis of C-poor subsoil horizons
- Combination of both methods: better understanding of SOM speciation and turnover

GRAPHICAL ABSTRACT

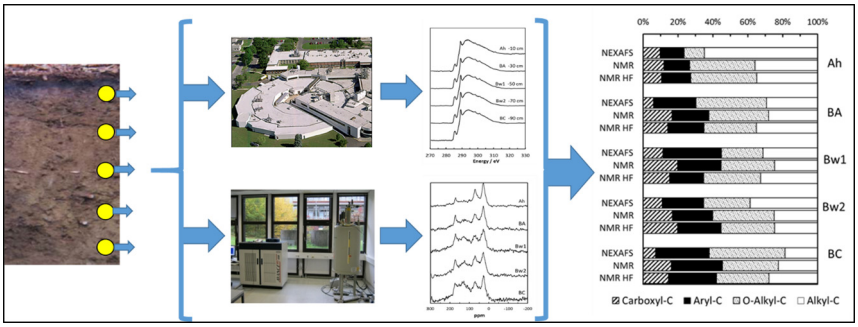

ABSTRACT

We compared synchrotron-based C near-edge X-ray absorption fine structure (NEXAFS) and CPMAS ^{13}C nuclear magnetic resonance (NMR) spectroscopy with respect to their precision and accuracy to quantify different organic carbon (OC) species in defined mixtures of soil organic matter source compounds. We also used both methods to quantify different OC species in organic surface horizons of a Histic Leptosol as well as in mineral topsoil and subsoil horizons of two soils with different parent material, stage of pedogenesis, and OC content (Cambisol: 15–30 OC mg g^{-1}, Podzol: 0.9–7 OC mg g^{-1}). CPMAS ^{13}C NMR spectroscopy was more accurate and precise (mean recovery of different C functional groups 96–103%) than C NEXAFS spectroscopy (mean recovery 92–113%). For organic surface and topsoil samples, NMR spectroscopy consistently yielded larger O-alkyl C percentages and smaller alkyl C percentages than C NEXAFS spectroscopy. For the Cambisol subsoil samples both methods performed well and showed similar C speciation results. NEXAFS spectroscopy yielded excellent spectra with a high signal-to-noise ratio also for OC-poor Podzol subsoil samples, whereas this was not the case for CPMAS ^{13}C NMR spectroscopy even after sample treatment with HF. Our results confirm the analytical power of CPMAS ^{13}C NMR spectroscopy for a reliable quantitative OC speciation in soils with >10 mg OC g^{-1}. Moreover, they highlight the potential of synchrotron-based C NEXAFS spectroscopy as fast, non-invasive method to semi-quantify different C functional groups in soils with low C content (0.9–10 mg g^{-1}).

1. Introduction

The chemical nature of soil organic matter (SOM), namely the speciation of soil organic carbon (SOC, OC), is a key soil property, reflecting

* Corresponding author.
E-mail address: prietzel@wzw.tum.de (J. Prietzel).

important SOM formation pathways as well as influencing ecological properties of humic topsoils (Cotrufo et al., 2015). Moreover, SOC speciation provides indicator properties for the SOM decomposition status (Baldock et al., 1997), as well as historic land-use (Chen et al., 2002), or vegetation (Prietzel et al., 2013). Therefore, a fast, accurate, and precise OC speciation in soils is desirable, and numerous methods (*e.g.* CPMAS ^{13}C NMR, Raman or FT-IR spectroscopy; gas chromatography, often after sample extraction, digestion, or derivatization) for the characterization of SOM are widely used. Most methods work fairly well for SOM-rich organic surface layers and humic topsoil horizons, but are less accurate in subsoil horizons with low SOM contents and/or large contents of pedogenic minerals (clay minerals; Fe, Al oxyhydroxides). With their large specific surfaces, these minerals interact strongly with SOM and often preferentially with particular C functional groups (O-alkyl C groups of polysaccharides; Schöning et al., 2005; Spielvogel et al., 2008). The presence of paramagnetic compounds (*e.g.* Fe oxyhydroxides) additionally results in signal broadening and functional group-specific quenching of CPMAS ^{13}C NMR signals, which bias SOM characterization at C:Fe ratios <1 (Arshad et al., 1988; Kögel-Knabner, 1997; Smernik and Oades, 2000; Schöning et al., 2005). Sample treatment with HF dissolves all minerals, resulting in SOM enrichment and removal of paramagnetic Fe oxyhydroxides (Skjemstad et al., 1994; Schmidt et al., 1997). However, it is still a matter of ongoing scientific debate (*e.g.* Sanderman et al., 2017), whether HF treatment yields a residual OM composition representing that before HF treatment or results in preferential removal of specific C functional groups with high affinity to soil oxyhydroxides (O-alkyl C; Schöning et al., 2005; Spielvogel et al., 2008). The deficit in available methods for a fast and reliable speciation of subsoil OM contrasts to the relevance of deep SOM for C sequestration and long-term OC storage in soils (Paul et al., 1997; Rumpel and Kögel-Knabner, 2011).

During recent decades, synchrotron-based X-ray spectroscopy has emerged as a powerful tool for soil analysis, allowing a direct, non-invasive speciation of many elements, including C, in soils (Lehmann and Solomon, 2010). Organic C speciation using this tool has been performed on soil extracts (Scheinost et al., 2001; Solomon et al., 2005; Christl and Kretzschmar, 2007), bulk soil samples (Jokic et al., 2003) and with sub-microspatial resolution also on soil aggregates and colloids (Wan et al., 2007; Lehmann et al., 2008; Keiluweit et al., 2012; Chen et al., 2014a, 2014b). These studies most often were qualitative, *i.e.* they fingerprinted OC speciation differences between soils, soil horizons, or aggregate regions rather than quantifying different C functional groups (*e.g.* Wan et al., 2007; Chen et al., 2014a, 2014b). Moreover, they mostly investigated SOM-rich topsoil rather than SOM-poor subsoil samples. Different C species in soils have also been quantified by C NEXAFS spectroscopy (*e.g.* Scheinost et al., 2001; Jokic et al., 2003; Solomon et al., 2005; Schumacher et al., 2005; Keiluweit et al., 2012). However, it is generally assumed that C NEXAFS spectroscopy performed on soils or soil extracts yields only "semi-quantitative" results, and that a quantitative interpretation of C NEAXFS spectra remains an unresolved challenge for several reasons summarized by Christl and Kretzschmar (2007).

With our study, we aimed to contribute to a reduction of the knowledge deficit concerning the ability of synchrotron-based C NEXAFS spectroscopy to quantify different soil C species. We investigated the accuracy and precision of C NEXAFS spectroscopy for the quantification of different C species in defined mixtures of organic compounds, which are enriched in particular C functional groups. Furthermore, we compared the accuracy and precision of C NEXAFS spectroscopy regarding the quantification of C functional groups in important SOM sources (lignin, cellulose, amino acids) with that of CPMAS ^{13}C NMR spectroscopy. Additionally, we compared the C speciation reported by both methods for surface, topsoil, and subsoil horizons of soils with different parent material, pedogenesis, and OC content.

2. Material and methods

2.1. Preparation of defined mixtures of organic compounds

We investigated the accuracy and precision of synchrotron-based C NEXAFS spectroscopy on two sample sets consisting of different defined mixtures of organic compounds. Set 1 comprised mixtures of four organic compounds specifically enriched in particular C functional groups or bonds between C atoms: **Graphite** (C_∞; consisting of solely aromatic C), **D-glucose** ($C_6H_{12}O_6$; solely O-alkyl C), **Ca formate** ($Ca[HCOO]_2$; solely carboxyl C), and ***L*-cysteine** ($C_3H_7NO_2S$; comprising carboxyl C, alkyl C, and C associated with amino or thiol groups). Set 2 comprised three major constituents of vascular plants, whose degradation products are considered important building blocks of SOM: **Cellulose** ($[C_6H_{10}O_5]_n$; 100% O-alkyl C), **lignin** ($C_9H_{10}O_2$,$C_{10}H_{12}O_3$,$C_{11}H_{14}O_4$; 61% aryl C; 30% O-alkyl C; 8% alkyl C; 1% carbonyl C), and ***L*-cysteine**, the latter representing proteins. Additionally, we included calcium carbonate ($CaCO_3$) as compound in Set 2 to test whether C NEXAFS spectroscopy can quantitate organic and inorganic C in calcareous soils. Cellulose (cotton linter; DP 7000) and lignin (spruce wood, "organocell" [ethanol/NaOH] processed) both were received from the Institute for Wood Research München, the other compounds were purchased from Sigma Aldrich. Seventeen different mixtures of graphite, glucose, *L*-cysteine, and Ca formate (Set 1) as well as 12 different mixtures of cellulose, lignin, *L*-cysteine, and $CaCO_3$ (Set 2) were prepared by careful homogenization in an agate ball Retsch minimill. Percentages of the different constituents in the mixing variants are presented on a C atom basis in Tables 1 and 2.

2.2. Selection and preparation of soil samples

We investigated the OC speciation of three German forest soils using C NEXAFS and CPMAS ^{13}C NMR spectroscopy. The soils differed in parent material, OC concentration, and content of pedogenic Fe minerals. Soil *Fall* (Table 3) is a Histic Leptosol ("Tangelrendzina"; Zech et al., 1985; Prietzel et al., 2013) formed on dolomite bedrock. It is located in the Bavarian Alps at an elevation of 1200 m a.s.l. and stocked with a mature *Picea abies–Abies alba* forest. Due to the cool and moist climate (MAT: 6.4 °C; MAP: 1767 mm), a thick organic surface layer (>40 cm) has accumulated on a shallow Ah horizon upon Triassic "Hauptdolomite" bedrock. From this soil, we sampled the organic surface layers (L, Of, Oh1, Oh2 horizons) and the Ah horizon. Soils *Mitterfels* and *Luess* are both stocked with mature *Fagus sylvatica* forest and have been studied intensively earlier (Lang et al., 2017; Werner et al., 2017a). *Mitterfels* is a Dystric Cambisol formed from Paleozoic gneiss. It is located in the Bavarian Forest at 1023 m a.s.l. The climate (MAT: 4.9 °C; MAP: 1300 mm) is less humid than that at *Fall*. The *Mitterfels* soil has a sand loam texture; it is acidic and has comparably high contents of OC (>15 mg g^{-1}) and Fe oxyhydroxides (Fe_d > 10 mg g^{-1}) in the entire mineral soil down to 90 cm depth (BC horizon; Table 3). We sampled the Ah, BA, Bw1, Bw2, and BC horizons of *Mitterfels*. Soil *Luess* is a Podzol formed from Pleistocene glaciofluvial outwash. It is located in N Germany in the Lüneburger Heide at 115 m a.s.l. Compared to *Fall* and *Mitterfels*, the climate at *Luess* is warmer and drier (MAT: 8.0 °C; MAP: 779 mm). The soil is characterized by a sandy texture, advanced podzolization (Werner et al., 2017a, 2017b) and low subsoil OC contents (<1 mg g^{-1}). We sampled the AE, Bh, Bs, Bw, and CB horizons down to 80 cm. After drying at 45 °C and sieving (<2 mm) the samples were finely ground, and their C speciation was analyzed by C NEXAFS and CPMAS ^{13}C NMR spectroscopy.

2.3. C NEXAFS spectroscopy

For nine pure C-bearing compounds, including those used for preparation of Sets 1 and 2, and additionally citric acid ($C_6H_8O_7$) as well as mannane ($C_{24}H_{42}O_{21}$), we acquired reference C NEXAFS spectra at the

Table 1
Results of C speciation of defined mixtures of organic C compounds with different functional C groups (Set 1) and important SOM sources (Set 2) as assessed by synchrotron-based C NEXAFS spectroscopy.

Set	Sample	Mixing ratio				Measured				Theoretical				Difference measured - theoretical			
		Glucose	Graphite	Cysteine	Ca formate	Carboxyl C	Aryl C	O-alkyl C	Alkyl C	Carboxyl C	Aryl C	O-alkyl C	Alkyl C	Carboxyl C	Aryl C	O-alkyl C	AlkylC
		% C				% C				% C				% C			
1	1	50	25	25	0	14	36	32	19	8	25	50	17	6	11	−18	2
1	2	25	25	50	0	18	31	33	19	17	25	25	33	1	6	8	−14
1	3	33	33	0	33	16	52	19	12	33	33	33	0	−17	19	−14	12
1	4	25	50	0	25	10	65	16	9	25	50	25	0	−15	15	−9	9
1	5	50	25	0	25	9	55	26	10	25	25	50	0	−16	30	−24	10
1	6	25	25	0	50	22	42	19	17	50	25	25	0	−28	17	−6	17
1	7	33	0	33	33	33	10	31	26	44	0	33	22	−11	10	−2	4
1	8	25	0	25	50	30	14	27	29	58	0	25	17	−28	14	2	12
1	9	25	25	25	25	15	31	34	19	33	25	25	17	−18	6	9	2
1	10	50	17	17	17	13	34	37	16	22	17	50	11	−9	17	−13	5
1	11	17	50	17	17	17	46	23	14	22	50	17	11	−5	−4	6	3
1	12	17	17	50	17	16	25	39	20	33	17	17	33	−17	8	22	−13
1	13	17	17	17	50	17	33	34	16	56	17	17	11	−39	16	17	5
1	14	70	10	10	10	14	29	42	15	13	10	70	7	1	19	−28	8
1	15	10	70	10	10	16	46	23	15	13	70	10	7	3	−24	13	8
1	16	10	10	70	10	19	24	38	20	33	10	10	47	−14	14	28	−27
1	17	10	10	10	70	36	23	19	22	73	10	10	7	−37	13	9	15
1	All samples: Mean value													−14	11	0	3
1	All samples: Standard deviation													13	12	16	11

Set	Sample	Mixing ratio				Measured					Theoretical					Difference measured - theoretical				
		Cellulose	Lignin	Cysteine	$CaCO_3$	Carboxyl C	Aryl C	O-alkyl C	AlkylC	$CO_3^{2-}C$	Carboxyl C	Aryl C	O-alkyl C	Alkyl C	$CO_3^{2-}C$	Carboxy lC	Aryl C	O-alkyl C	Alkyl C	$CO_3^{2-}C$
		% C				% C					% C					% C				
2	1	33	33	33	0	11	37	28	24	0	12	20	43	25	0	−1	17	−15	−1	0
2	2	25	50	25	0	8	38	23	31	0	9	30	40	21	0	−1	8	−17	10	0
2	3	50	25	25	0	13	36	28	24	0	9	15	58	19	0	4	21	−30	5	0
2	4	25	25	50	0	17	32	28	23	0	17	15	33	35	0	0	17	−5	−12	0
2	5	25	25	25	25	13	29	21	31	6	9	15	33	19	25	4	14	−12	12	−19
2	6	50	17	17	17	23	44	26	2	6	6	10	55	12	17	17	34	−29	−10	−11
2	7	17	50	17	17	7	29	10	51	2	6	30	32	15	17	1	−1	−22	36	−15
2	8	17	17	50	17	26	34	25	4	10	17	10	22	35	17	9	24	3	−31	−7
2	9	17	17	17	50	12	22	19	39	8	6	10	22	12	50	6	12	−3	27	−42
2	10	70	10	10	10	11	21	19	40	8	3	6	73	7	10	8	15	−54	33	−2
2	11	10	70	10	10	18	51	14	1	15	4	42	31	12	10	14	9	−17	−11	5
2	12	10	10	70	10	15	18	34	33	0	23	6	13	47	10	−8	12	21	−14	−10
2	All samples: Mean value															4	15	−15	4	−8
2	All samples: Standard deviation															7	9	19	21	13
1 + 2	All samples: Mean value															−7	13	−6	4	−8
1 + 2	All samples: Standard deviation															14	11	19	16	13

NIST U7A beamline of the National Synchrotron Light Source (NSLS) 1 storage ring (2.8 GeV) located at the Brookhaven National Laboratory, Upton, NY, USA. Thereafter, we obtained spectra for all Set 1 and Set 2 mixtures and the soil samples. We firmly pressed all samples into a Cu tape mounted on a sample holder. After 12 h desiccation under vacuum, NEXAFS spectra were acquired under vacuum at the C K-edge (energy range: 270–340 eV; energy resolution: 0.25 eV; X-ray spot size at sample: 1 mm^2). The monochromator (toroidal spherical grating monochromator; $\Delta E/E$: $2 * 10^{-4}$) was calibrated daily with a carbon mesh downstream of the monochromator. We acquired spectra in Partial Electron Yield (PEY) mode using a channeltron electron multiplier with an entrance grid voltage of −50 V. The incident beam intensity, I_0, was measured concomitantly using a clean gold mesh located upstream of the samples. For each sample, we acquired two spectra. Without exception, the two spectra agreed perfectly with each other, which assured that no radiation damage and C speciation change has occurred during spectra acquisition. Prior to base-line correction, edge-step normalization, merging, and deconvolution, all spectra were corrected for I_0 to give (signal[energy] = PEY[energy] / I_0[energy]).

According to the spectra obtained for the reference compounds, the energies of the Gaussian peaks G1–G6 produced by six major C electron transition groups of soil OC constituents as described earlier (*e.g.* Cody et al., 1998; Scheinost et al., 2001; Solomon et al., 2005; Lehmann et al., 2009) were identified as shown in Table 4. Additionally, another Gaussian peak G7 at 290.7 eV was assigned to carbonate C. Merging of the two spectra acquired for each sample as well as base-line correction, edge-step normalization, and deconvolution of all spectra was performed using the software ATHENA (Ravel and Newville, 2005) of the DEMETER package (Version 0.9.25). After base-line correction (energy range: 270–275 eV) and edge-step normalization (energy range: 320–340 eV), the spectra of all mixtures and soil samples were deconvoluted in the energy range 270–294 eV according to Solomon et al. (2005) using the procedure *peakfit* in ATHENA. We fitted one arctan function (energy 290.4 eV; height 1; FWHM 0.5 eV) representing the edge step. Then we fitted the Gaussian peaks G1–G6 (G1–G7 if carbonate was assumed to be present in a sample), and two Gaussian peaks at 292 and 294 eV, representing broad additional 1s → σ* transitions of saturated single covalent bonds and direct inner-shell ionization (Scheinost et al., 2001; Solomon et al., 2005). The FWHMs of the Gaussian peaks were initially set to 0.4 eV (G1–G7) and 1 eV (other Gaussian peaks), and their heights set to the value 1, but allowed to float during later stages of spectrum deconvolution. Assuming identical specific X-ray absorption coefficients for all C species, we calculated the contribution of different C species (aryl C, alkyl C, O-alkyl C, carboxyl C, carbonate C) as quotient of the area of their respective Gaussian peaks (Table 4) G1 + G2 + G3, G4, G5, G6, G7 divided by the sum of the areas of peaks G1 to G7.

2.4. Solid state CPMAS ^{13}C NMR spectroscopy

For the Set 2 mixtures and soil samples, we additionally acquired solid state ^{13}C NMR spectra using a BRUKER DSX 200 NMR spectrometer (resonance frequency: 50.323 MHz, Bruker Corp. Rheinstetten, Germany), applying the CPMAS technique (Schaefer and Stejskal, 1976). We rotated the samples at the magic angle (54.78°) with a spinning speed of 6.8 kHz to avoid line broadening due to orientation-dependent interactions (Wilson, 1987). We collected the spectra with a 700 ms pulse delay and used a ramped ^1H-pulse during a contact time of 1 ms to circumvent Hartmann-Hahn mismatches (Peersen et al., 1993). Depending on sample sensitivity, the number of accumulated scans ranged between 10,000 and 100,000. We used a line broadening between 10 and 15 Hz before Fourier transformation to improve the signal-to-noise ratio. The chemical shift is given relative to tetramethylsilan (50 ppm), calibrated with glycine (176.03 ppm). To quantify different C species we divided each spectrum into four chemical shift regions, which represent specific C functional groups (Wilson, 1987; Knicker and Lüdemann, 1995; Kögel-Knabner, 1997): The chemical shift region −10–45 ppm represents alkyl-C, including lipids, cutin, and amino acids. The region 45–110 ppm represents O/N-alkyl C, including carbohydrates, cellulose, methoxyl C, C—N of amino acids, and hemicellulose. The region 110–160 ppm represents aryl C, including lignin, tannin, aromatic compounds, olefines, and the region 160–220 ppm represents carboxyl/amide and carbonyl C, including carboxylic acids, amide, aldehyde, and ketone. All NMR spectra were manually baseline corrected and phased; subsequently we quantified the respective areas by integration. In soils with C/Fe ratios <1, paramagnetic Fe (*e.g.* in Fe oxyhydroxides) confounds the NMR-spectroscopic assessment of different C species by signal broadening and shortening the relaxation times of C atoms depending on their affinity to paramagnetic centers. This results in underestimation of certain C structures (Arshad et al., 1988; Skjemstad et al., 1997; Smernik and Oades, 2000; Schöning et al., 2005). We therefore treated mineral soil subsamples with 10% (v/v) HF before NMR spectroscopy (Schmidt et al., 1997) to remove paramagnetic minerals and increase the SOC concentration in the residue. Ten g of ground sample were shaken with 50 mL HF for 2 h; then we centrifuged it at 48 °C and removed the supernatant. The procedure was repeated five times; then the sediment was washed five times with 50 mL deionized water and freeze-dried.

3. Results

3.1. Defined mixtures of C-bearing compounds

The edge-step-normalized C NEXAFS spectra of the pure endmembers graphite, *L*-cysteine, Ca formate, and glucose in Set 1 of our mixture study (100Gr, 100Cy, 100CF, and 100Gl, respectively) differed markedly from each other and showed the typical peaks of their specific C functional groups (Fig. 1a–d). Moreover, spectra with different (25%, 50%, 70%, 100%) enrichment grades of graphite (Fig. 1a), *L*-cysteine (Fig. 1b), Ca formate (Fig. 1c), or glucose (Fig. 1d) in quaternary mixtures of these four compounds differed systematically, with peaks of increasingly enriched C species increasing in intensity. The C NEXAFS (Fig. 2) and NMR spectra (Fig. 3) acquired for the ternary mixtures of Set 2, comprising the SOM source compounds lignin, *L*-cysteine (proxy for proteins), and cellulose, also well reflected the respective abundances of aryl, alkyl, O-alkyl, and carboxyl C functional groups. For C NEXAFS spectroscopy, different percentages of carbonate C were evident in the spectra (Fig. 2b), whereas carbonate C was not detected by CPMAS ^{13}C NMR spectroscopy (Fig. 3b) due to the absence of ^1H atoms in carbonate (Kinchesh et al., 1995).

The contributions of different C functional groups to total C in the 29 mixtures of Sets 1 and 2 as calculated by deconvolution of the respective C NEXAFS spectra on average agreed well with the respective expected contributions (Table 1). For seven out of nine investigated C functional group × Set combinations, obtained recoveries were proven to be normally-distributed by a Kolmogorov–Smirnov test with variance correction according to *Lillefors*, allowing the use of arithmetic mean values and standard deviation for the characterization of recovery patterns. For Set 1, the contribution of carboxyl C to total C in the mixtures on average was underestimated 14%. The contributions of aryl C and alkyl C on average were overestimated 11% and 3%, respectively. The contribution of O-alkyl C on average was reported correctly. For Set 2, O-alkyl C and carbonate C on average were underestimated 15% and 8%, respectively. Carboxyl C and alkyl C on average each were overestimated 4% and aryl C was overestimated 15%. Both sets pooled, C NEXAFS spectroscopy on average underestimated carboxyl C, O-alkyl C, and carbonate C 7%, 6%, and 8% respectively and overestimated alkyl C and aryl C 4% and 13%, respectively (Table 1). Underestimation of a specific C functional group was as large as 54% (O-alkyl C in sample 10 of Set 2); overestimation was up to 36% (alkyl C in sample 7 of Set 2). Underestimation of a specific C functional group generally was largest for mixtures with high enrichment of that group.

Table 2
Results of C speciation of defined mixtures of important SOM sources (Set 2) as assessed by CPMAS ^{13}C NMR spectroscopy. ND: Not determined.

Set	Sample	Mixing ratio				Measured					Theoretical					Difference measured - theoretical				
		Cellulose	Lignin	Cysteine	$CaCO_3$	Carboxyl C	Aryl C	O/N-alkyl C	Alkyl C	CO_3^{2-} C	Carboxyl C	Aryl C	O/N-alkyl C	Alkyl C	CO_3^{2-} C	Carboxyl C	Aryl C	O/N-alkyl C	Alkyl C	CO_3^{2-} C
		% C				% C					% C					% C				
2	1	33	33	33	0	7	25	55	13	ND	12	20	54	14	0	−5	5	0	0	ND
2	2	25	50	25	0	8	32	47	14	ND	9	30	48	12	0	−1	2	−2	1	ND
2	3	50	25	25	0	7	20	61	12	ND	9	15	66	10	0	−2	5	−5	1	ND
2	4	25	25	50	0	11	21	49	19	ND	17	15	49	19	0	−6	6	0	1	ND
2	5	25	25	25	25	6	26	52	16	ND	12[a]	20[a]	54[a]	14[a]	(25)	−5	5	−3	2	ND
2	6	50	17	17	17	5	15	69	10	ND	7[a]	12[a]	73[a]	8[a]	(17)	−2	3	−4	2	ND
2	7	17	50	17	17	6	38	42	14	ND	8[a]	37[a]	45[a]	12[a]	(17)	−2	1	−3	3	ND
2	8	17	17	50	17	12	14	53	20	ND	20[a]	12[a]	46[a]	22[a]	(17)	−8	2	7	−2	ND
2	9	17	17	17	50	7	26	51	15	ND	12[a]	20[a]	55[a]	14[a]	(50)	−4	6	−4	2	ND
2	10	70	10	10	10	3	9	81	6	ND	4[a]	7[a]	85[a]	5[a]	(10)	−1	2	−3	2	ND
2	11	10	70	10	10	5	45	37	13	ND	5[a]	47[a]	38[a]	10[a]	(10)	0	−2	−1	3	ND
2	12	10	10	70	10	21	8	43	29	ND	26[a]	7[a]	40[a]	27[a]	(10)	−6	1	3	2	ND
2	All samples: Mean value															−4	3	−1	1	–
2	All samples: Standard deviation															3	2	3	1	–

[a] Percentages add to 100 with carbonate-C set to 0.

Table 3
Important chemical properties of the soil samples. OC: Organic carbon. Fe_d: Dithionite-citrate-bicarbonate-extractable Fe according to Mehra and Jackson (1960). Fe_o, Al_o: Oxalate-extractable Fe and Al according to Schwertmann (1964). ND: Not determined.

	OC	Fe_d	Fe_o	Al_o
	mg g^{-1}			
Histic Leptosol *Fall*				
L	481	ND	ND	ND
Of	457	0.8	0.3	0.2
Oh1	435	1.7	1.4	1.6
Oh2	397	8.0	4.7	4.0
Ah	100	11.3	7.2	3.4
Dystric Cambisol *Mitterfels*				
Ah	74.5	18.0	10.3	3.3
BA	32.8	12.9	7.4	5.3
Bw1	24.6	11.6	6.4	7.8
Bw2	16.8	10.7	5.2	6.9
BC	15.7	10.1	3.6	5.6
Haplic Podzol *Luess*				
AE	57.6	1.4	1.0	0.7
Bh	4.9	3.8	1.5	0.4
Bs	6.4	5.5	1.3	2.1
Bw	1.2	2.3	0.3	0.6
CB	0.9	2.5	0.2	0.4

We did not quantify the contribution of different C functional groups to total C in the Set 1 mixtures, because Set 1 included compounds (graphite, glucose) inaccessible to CPMAS ^{13}C NMR spectroscopy. The contributions of different C functional groups to total C in the 12 ternary and quaternary mixtures of Set 2 as calculated by deconvolution of the respective CPMAS ^{13}C NMR spectra on average excellently agreed with the expected contributions (Table 2). For Set 2, after correction for the carbonate C percentage, which showed no signal in the NMR spectra (Fig. 3b), carboxyl C on average was underestimated 4%, O/N-alkyl C on average was underestimated 1%. Alkyl C on average was overestimated 1%, and aryl C overestimated 3% (Table 2). The overall accuracy of ^{13}C NMR spectroscopy, calculated as sum of the squared average percent under- or overestimation values of the four C species in all samples of Set 2 was 27 and much better than that of C NEXAFS spectroscopy (482). Even more so, the precision, calculated as sum of squared standard deviations of the mean recoveries of the four investigated C species in Set 2, was much better for ^{13}C NMR spectroscopy (23) compared to C NEXAFS spectroscopy (932). In the NMR assessments, underestimation of a specific C functional group could be as large as 8% (carboxyl C in sample 8 of Set 2), and maximum overestimation of a specific C functional group was 7% (O/N-alkyl C in the same sample). Compared to C NEXAFS spectroscopy, CPMAS ^{13}C NMR spectroscopy on average yielded smaller contributions of carboxyl C, aryl C, and alkyl C, and larger O/N-alkyl C contributions in the Set 2 mixtures.

3.2. Organic surface soil samples

Both C NEXAFS and ^{13}C NMR spectra obtained on the samples from the Histic Leptosol *Fall*, which have large OC concentrations (L, O layers: >390 mg g^{-1}; Ah: 100 mg g^{-1}) and wide OC/Fe_d ratios (Table 5), were characterized by a high signal-to-noise ratio and clear signals indicative for specific OC functional groups (Fig. 4a,b). The spectra indicate a large contribution of O-alkyl C (NEXAFS: 289.8 eV; NMR: 45–110 ppm) and alkyl C (NEXAFS: 288.2 eV; NMR: −10–45 ppm) to total C in all samples. With C NEXAFS spectroscopy, consistently smaller percentages of O-alkyl C and larger percentages of alkyl C, carboxyl C, and aryl C (exception: L) were measured than with ^{13}C NMR spectroscopy (Fig. 4c).

Table 4
Peak energies of Gaussian Peaks G1–G6 as assigned to different C 1s electron transitions and organic C forms by Lehmann et al. (2009).

Peak	Peak energy [eV]	Organic C forms	Bond	Transition	C compounds (examples)
G1	284.9	Aromatic C Quinone C	C═O	1s ➔ π*	Quinone-type C, protonated or alkylated aromatic C, Heteroatom substituted aromatic C
G2	285.4	Aromatic C Double-bonded alkyl C	C═C	1s ➔ π*	Protonated or alkylated aromatic C Carbonyl substituted aryl C Alkene C
G3	287.3	Aromatic C with side chain N-substituted aromatic C	C—OH C═O R—(C═O)—R′ C═N, C—N	1s ➔ π*	Carbonyl C in aromatic ring Aromatic C attached to amide group Phenol C, carbonyl C, pyrimidine C
G4	288.2	Aliphatic C (***Alkyl C***)	C—H	1s ➔ 3p/σ*	Aliphatic C of CH_3, CH_2, and CH nature
G5	289.0	Aliphatic C (***Carboxyl C***)	R—COOH COO C═O NH_2—C—O R—(NH_2)—R′	1s➔π*	Carboxylic C Carboxylamide C Carbonyl C
G6	289.8	Aliphatic C (***O-alkyl C***)	C—OH	1s ➔ π* 1s ➔ 3p/σ*	Polysaccharides, alcohols, Other hydroxylated and ether-linked C

3.3. Mineral soil samples

3.3.1. Quality of C NEXAFS and ^{13}C NMR spectra

For all mineral soil horizons of *Mitterfels* (OC concentration: 16–75 mg g^{-1}; Table 3; OC/Fe_d ratio in B horizons 1.6–2.5; Table 5) and *Luess* (OC concentration: 0.9–58 mg g^{-1}; OC/Fe_d ratio in B and CB horizons 0.4–1.3) excellent spectra with a good signal-to-noise ratios were acquired by C NEXAFS spectroscopy (Fig. 5a,e). The quality of the ^{13}C NMR spectra was good for the mineral topsoil (Ah, AE) samples of *Mitterfels* and *Luess* (OC >50 mg g^{-1}; OC/Fe_d ratio > 4). However, it was worse for the subsoil samples of *Mitterfels* (increased noise and increased interference by paramagnetic Fe; Fig. 5b), and poor (low signal-to-noise ratios; strong signal broadening by paramagnetic Fe; Fig. 5f) for most subsoil samples of *Luess*. Sample treatment with HF resulted in improved spectrum quality (noise reduction, decrease of Fe interference) for the Bw, but not the BC horizon samples of *Mitterfels* (Fig. 5c), whereas no marked improvement was achieved for *Luess* subsoil samples (Fig. 5g).

3.3.2. C speciation of the Mitterfels Cambisol

According to the C NEXAFS spectroscopy results (Fig. 5d), alkyl C predominates as C functional group in the SOM of the *Mitterfels* Ah horizon, comprising 65% of total C. The other C species each contribute 10–15% to SOC. In the *Mitterfels* B horizons, without a systematic depth trend of C speciation, the contribution of alkyl C to total C ranges between 30 and 40%, that of O-alkyl C between 25 and 40%, and that of aryl C between 25 and 35%. With a contribution between 6 and 12%, carboxyl C is of minor relevance in the entire profile. In the *Mitterfels* BC horizon most C is O-alkyl C (43% of total C) or aryl C (31% of total C).

Similar to *Fall*, also in the *Mitterfels* Ah horizon the OC speciation as reported by ^{13}C NMR spectroscopy differs markedly from that reported by C NEXAFS spectroscopy (Fig. 5d). The contribution of O-alkyl C to total OC with 37% is much larger, that of alkyl C (36%) much smaller. For the B and BC horizons of *Mitterfels*, in most cases the OC speciation as reported by C NEXAFS and ^{13}C NMR spectroscopy is similar (Fig. 5d), except a consistently larger contribution of carboxyl C and smaller alkyl C and aryl C contributions reported by ^{13}C NMR compared to C NEXAFS spectroscopy. HF treatment of the *Mitterfels* B horizon samples in most cases resulted in some change of their OC speciation (Fig. 5d). The contribution of alkyl C to total C increased, and the contribution of carboxyl C and aryl C decreased slightly, resulting in an increase of the alkyl C/O-alkyl C ratio (Table 5).

3.3.3. C speciation of the Luess Podzol

As for the Ah horizons of the other two soils, also for the SOM in the *Luess* AE horizon a predominance of alkyl C (52% of total C) was reported by C NEXAFS spectroscopy (Fig. 5h). O-alkyl C was 21%, aryl C and carboxyl C were 0–15% of SOC. With soil depth, the contribution of alkyl C to total C as reported by C NEXAFS spectroscopy generally decreased (exception: Bh horizon), but was >40% of total C even in the lowermost horizon. With 25–35% of total C in most horizons of *Luess* O-alkyl C was the second most relevant C species. The *Luess* Bs horizon differed from all other horizons by a low contribution of alkyl C to total C (11%) and particularly large contributions of aryl C (39%) and carboxyl C (24%). Compared to the Ah horizons the other two soils, the OC speciation as reported by ^{13}C NMR spectroscopy for the AE horizon of the Podzol *Luess* differed much less from that reported by C NEXAFS spectroscopy (larger contribution of O-alkyl C; smaller contribution of alkyl C; Fig. 5h). In contrast to the *Mitterfels* B horizons, however, in the *Luess* B and BC horizons the OC speciation reported by C NEXAFS spectroscopy differed markedly from that reported by ^{13}C NMR spectroscopy. Except the Bs horizon, the contribution of alkyl C to total C always was considerably lower (<16%; C NEXAFS spectroscopy: >40% of total C), and the contributions of carboxyl C and aryl C in most cases were markedly larger. HF treatment neither did markedly change the OC speciation of the *Luess* AE horizon sample nor systematically affected the OC speciation of the *Luess* subsoil samples.

4. Discussion

4.1. Quantification of C functional groups in mixtures of organic C compounds

Our results showed that C NEXAFS spectroscopy is less accurate and particularly less precise than CPMAS ^{13}C NMR spectroscopy in quantifying the contribution of different C functional groups to total C in mixtures of organic compounds considered as relevant SOM sources. The average recovery of many NEXAFS analyses performed on a large number of samples was good (mean recovery of different C functional groups: 92–113%; Table 1). According to these results, different X-ray absorption coefficients among functional C groups (larger for C-1s ➔ π* transitions of aryl C and carboxyl C; smaller for C-1s ➔ 3p/σ* transitions of alkyl C and O-alkyl C; *e.g.* Stöhr, 1996; Christl and Kretzschmar, 2007) at least in our mixtures did not seriously compromise the mean accuracy of the C speciation using C NEXAFS spectroscopy. However, particularly for the C speciation of **a single sample**, CPMAS ^{13}C NMR spectroscopy was more accurate and precise than C NEXAFS spectroscopy. CPMAS ^{13}C NMR spectroscopy always correctly reported the expected percentages of alkyl C (Fig. 6a; recovery 101 ± 1%) and O/N-alkyl C (Fig. 6b; recovery 99 ± 3%; amino C of *L*-cysteine was assigned to the O-alkyl C region). Aryl C was also quantitated with good accuracy and precision (Fig. 6c; recovery 103 ± 2%). Carboxyl C (recovery 96 ±

3%) was considerably underestimated at true percentages >10% (Fig. 6d). This is probably due to the circumstance that carboxyl C is remote from protons and thus less enhanced than other moieties by cross polarization (Simpson et al., 2012).

The unsatisfactory performance of C NEXAFS spectroscopy to quantify exactly the contribution of different C functional groups in our mixtures on a single-sample level is evident in Fig. 6e–h. Particularly alkyl C (Fig. 6e) and O-alkyl C (Fig. 6f), were recovered with poor precision (alkyl C: 104 ± 16%; O-alkyl C: 94 ± 19%) and generally overestimated at true percentages <25% of total C, but underestimated at true percentages >25% of total C. This is also the case with carboxyl C (Fig. 6h; recovery 93 ± 14%). Aryl C in most cases was overestimated by C NEXAFS spectroscopy (Fig. 6g; recovery 113 ± 11%), which may be due to the larger X-ray absorption coefficient of 1s ➔ π* transitions of aryl C compared to the C-1s ➔ 3p/σ* transitions of alkyl C and O-alkyl C (Stöhr, 1996; Christl and Kretzschmar, 2007). A possible cause for the low precision of C NEXAFS spectroscopy, despite generally good spectra quality (*i.e.* high signal-to-noise ratios) is the fact that the signals produced in the spectra by the different C functional groups are much less pronounced compared to the signals produced by the same groups in CPMAS ^{13}C NMR spectra. Particularly the Rydberg transition of the alkyl C functional group does not produce a distinct peak-shape signal 288.2 eV even at high concentration (*e.g.* 100Cy spectrum in Fig. 1b). It merely produces a shoulder whose correct and reliable fitting by a Gaussian peak is confounded by the shape and magnitude of the nearby carboxyl C signal at 289 eV (Cody et al., 1998; Scheinost et al., 2001; Solomon et al., 2005; Christl and Kretzschmar, 2007). Moreover, assigning different C functional groups to the G1–G6 peaks presented in Table 4, as traditionally performed in SOC speciation studies using

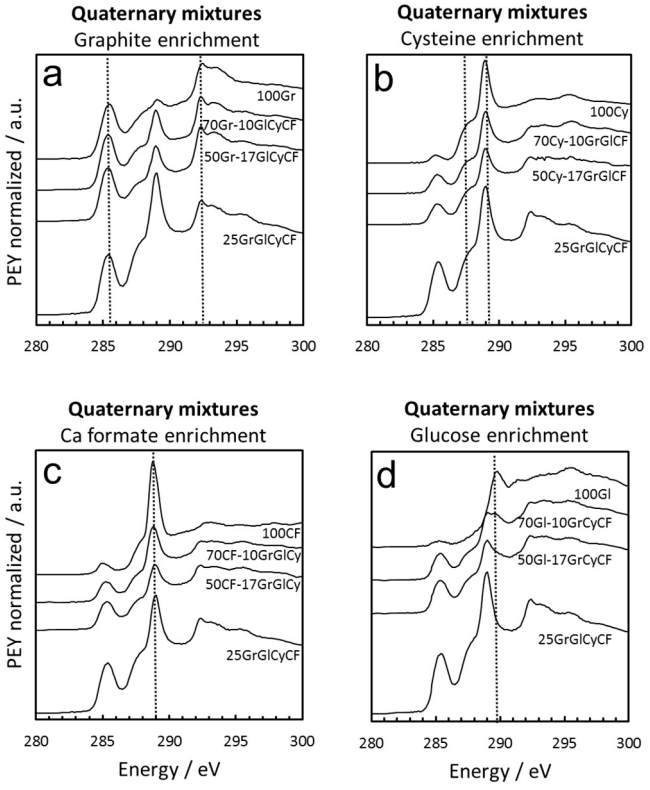

Fig. 1. Normalized C NEXAFS spectra of different quaternary mixtures with enrichment of (a) graphite [Gr], (b) *L*-cysteine [Cy], (c) calcium formate [*CF*], and (d) glucose [Gl]. Number before compound symbol: Percent contribution of this compound to mixture. Dotted lines indicate specific energies of C functional group signals in the respective compound enriched in the mixtures. Example 50Gr-17GlCyCF: Mixture with 50% of total C present as graphite-C, 17% of total C present as glucose-C, Cysteine-C, and calcium formate-C, respectively.

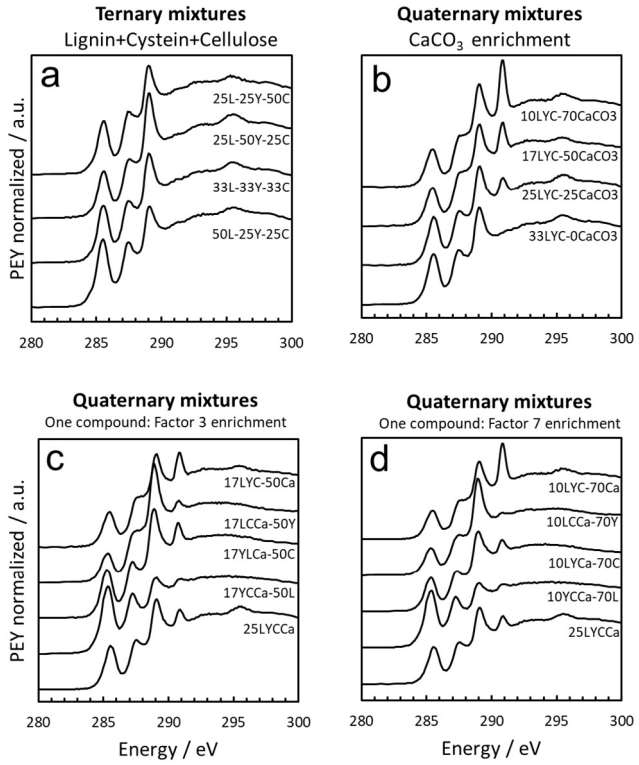

Fig. 2. Normalized C NEXAFS spectra of different ternary and quaternary mixtures of lignin (L), cysteine (Y), cellulose (C), and calcium carbonate ($CaCO_3$, Ca). Number before compound symbol: Percent contribution of this compound to the mixture. Example 25L-25Y-50C: Mixture with 25% of total C present as lignin-C, 25% of total C present as cysteine-C, and 50% of total C present as cellulose-C.

NEXAFS spectroscopy (*e.g.* Cody et al., 1998; Solomon et al., 2005; Lehmann et al., 2008) is only an approximation to the truth. The NEXAFS signal of a specific C functional group can vary in peak energy and shape depending on the structure of adjacent C groups (Scheinost et al., 2001; Kaznacheyev et al., 2002; Christl and Kretzschmar, 2007). The same is true for the NEXAFS signals produced by ionization of the core C atoms of different C functional groups which for the sake of simplicity in our spectrum deconvolution protocol all are represented by one single arctan function ("edge step") with fixed energy (290.4 eV) and width (0.5 eV). More sophisticated C NEXAFS spectra deconvolution techniques may result in improved accuracy and precision of quantitative SOC speciation by C NEXAFS spectroscopy (Heymann et al., 2011).

In contrast to the mineral mixtures, the C speciation results reported for the organic surface layers of *Fall* (Fig. 4c) show no erratic patterns, but a systematic C speciation change with soil depth. This suggests that the unsatisfactory precision of C NEXAFS spectroscopy for analysis of the C speciation in our defined organic mixtures may not primarily be due to low accuracy and/or precision of the NEXAFS analysis itself. We assume that incomplete homogenization of the mixture constituents during the mixing procedure is a key issue. As considerably smaller mixture subsample amounts (<10 mg) were used for NEXAFS compared to NMR spectroscopy (up to one gram), millimeter-scale inhomogeneity of the mixtures probably has affected NEXAFS more than NMR spectroscopy results. If the poor precision of C NEXAFS spectroscopy indeed is largely due to millimeter-scale sample heterogeneity effects, it should be much better for natural organic matter (*e.g.* plant residues). The latter consists of closely associated, often chemically bound assemblages of organic compounds with different C functional groups (*e.g.* lignocellulose consisting of lignin-cellulose moieties rather than separated lignin and cellulose molecules), whose spatial heterogeneity scale is much smaller than the irradiated sample area (1 mm^2 at beamline U7A). The spatial scale of C functional group heterogeneity is even smaller

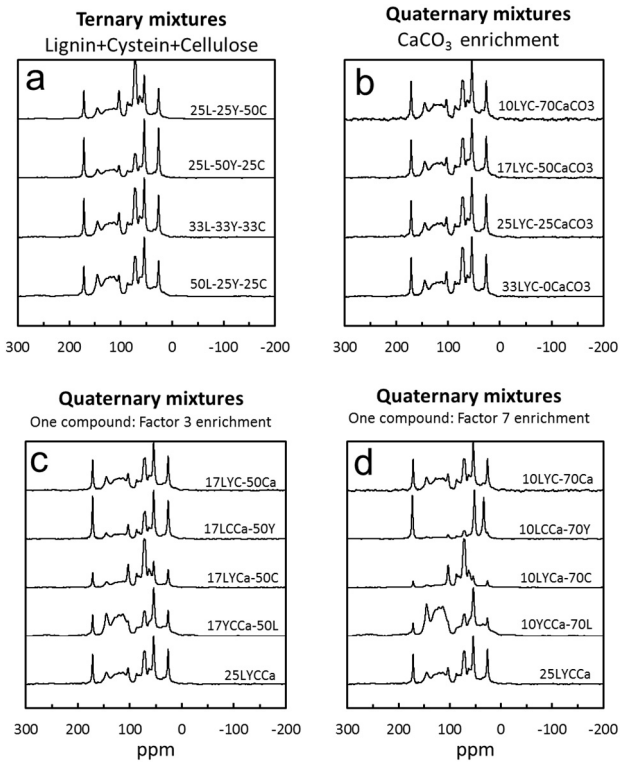

Fig. 3. CPMAS ^{13}C NMR spectra of different ternary and quaternary mixtures of lignin (L), cysteine (Y), cellulose (C), and calcium carbonate ($CaCO_3$, Ca). Number before compound symbol: Percent contribution of this compound to the mixture. O-alkyl C fraction quantitated by NMR spectroscopy includes also N-alkyl C. Example 17LYC-50Ca: Mixture with 50% of total C present as calcium carbonate, and 17% of total C present as lignin-C, Cysteine-C, and cellulose-C, respectively.

for SOM, consisting of different organic domains closely arranged in submicron assemblages (Lehmann et al., 2008).

NEXAFS spectroscopy overestimated O-alkyl C for true percentages <25% of total OC (Fig. 6f) in the Set 2 mixtures, whereas CPMAS ^{13}C NMR spectroscopy always quantified O-alkyl C correctly (Fig. 6b). Yet, for all Set 2 samples, larger O-alkyl C contributions to total C were reported with NMR compared to NEXAFS spectroscopy (Fig. 6j). This systematic discrepancy can be partly explained by the fact that C bound to amino groups of *L*-cysteine in our spectra evaluation contributes to the O-alkyl C (correctly: O/N-alkyl C) chemical region in NMR spectra, but not in C NEXAFS spectra. *L*-cysteine produces a signal with a chemical shift of 54 ppm (Fig. 3) and is a major constituent of many Set 2 samples. Yet, NMR spectroscopy reported only little more O-alkyl C than NEXAFS spectroscopy for the Set 2 samples 4, 8, and 12 (Fig. 6j; gray symbols), which are characterized by particularly large contributions of *L*-cysteine (50%, 50%, and 70% of total C in the respective mixtures; Table 1). This finding indicates that the different assignment of N-alkyl C by both methods is a minor issue for the reported underestimation of O-alkyl C by NEXAFS compared to NMR spectroscopy in our mixtures. Larger contributions of aryl C reported by NEXAFS compared to ^{13}C NMR spectroscopy for most Set 2 samples (Fig. 6k) can be attributed to the systematic overestimation of this C functional group by NEXAFS spectroscopy (Fig. 6g). The overestimation of carboxyl C by NEXAFS compared to NMR spectroscopy (Fig. 6l) was due to overestimation of this C species with NEXAFS at true percentages <25% of total OC (Fig. 6h) and the carboxyl C underestimation by CPMAS ^{13}C NMR spectroscopy at true percentages >10% (Fig. 6d). In our study, the percentages of different C functional groups in the Set 2 mixtures as reported by NEXAFS compared to NMR spectroscopy showed no significant correlation (*r*: 0.01–0.53; Fig. 6i–l). In contrast to our results, Scheinost et al. (2001) and Solomon et al. (2005) reported markedly larger positive correlations between the percentages of different C species quantified by

Table 5
Organic carbon (OC)/Fe_d (dithionite-bicarbonate-citrate extractable Fe; Mehra and Jackson, 1960) mass ratio, and alkyl C/O-alkyl C ratio* in different horizons of Histic Leptosol *Fall*, Cambisol *Mitterfels*, and Podzol *Luess* as quantified by C NEXAFS and CPMAS ^{13}C NMR spectroscopy. ND: Not determined.

Soil	Horizon	OC/Fe_d	Alkyl C/O-alkyl C ratio*			Mass loss	OC loss
			NEXAFS	NMR	NMR		
					After HF treatment	After HF treatment	After HF treatment
Fall	L	ND	1.75	0.32	ND	ND	ND
	Of	571.3	1.38	0.37	ND	ND	ND
	Oh1	255.9	1.19	0.40	ND	ND	ND
	Oh2	49.6	1.28	0.42	ND	ND	ND
	Ah	8.8	8.85	0.56	ND	ND	ND
Mitterfels	Ah	4.1	5.59	0.96	0.93	47%	ND
	BA	2.5	0.72	0.82	1.17	96%	53%
	Bw1	2.1	1.31	0.81	1.01	81%	41%
	Bw2	1.6	1.47	0.70	0.81	93%	62%
	BC	1.6	0.43	0.70	0.93	82%	46%
Luess	AE	41.1	2.43	1.17	1.20	ND	8%
	Bh	1.3	6.91	0.52	0.51	49%	71%
	Bs	1.2	0.47	0.75	0.73	52%	71%
	Bw	0.5	1.50	0.36	0.45	80%	89%
	CB	0.4	1.23	0.13	0.47	49%	69%

*NMR spectroscopy: ratio alkyl C/(O-alkyl C plus N-alkyl C).

NEXAFS and by NMR spectroscopy in alkaline soil extracts. This supports our assumption, that the low accuracy and/or precision of NEXAFS in our study is largely due to incomplete homogenization of the mixture constituents during the mixing procedure.

In summary, CPMAS ^{13}C NMR spectroscopy with our instrumental setting and spectrum deconvolution method accurately and precisely quantitated all C functional groups except carboxyl C on a wide range of true percentages in our Set 2 mixtures, which comprised major SOM sources (lignin, cellulose, amino acids), and which were characterized by large OC concentrations and absent interference by paramagnetic compounds. Carbon NEXAFS spectroscopy is less accurate and particularly less precise than ^{13}C NMR spectroscopy, but offers the possibility for a simultaneous estimation of carbonate C coexisting with OC. It must, however, be emphasized that the accuracy and precision of both methods in real soils may differ from that quantified for our defined mixtures. First, we indeed conducted our accuracy and precision assessments on organic compounds that are major SOM sources; however, in soil environments these compounds become rapidly modified by numerous biochemical processes. Therefore, SOM consists of a multitude of different organic compounds and organo-mineral assemblages, each possibly characterized by a specific X-ray absorption fine structure, depending on substitution of C atoms or neighboring C functional groups (Christl and Kretzschmar, 2007; Solomon et al., 2009). Moreover, uncertainties in absolute intensity response of electron transitions, strongly overlapping resonance ranges of electron transitions, effects of σ^* and π^* bond-bond interactions, and bond-dependent positions of ionization potential seriously challenge an accurate and precise quantification of different C species in soils by NEXAFS spectroscopy (Christl and Kretzschmar, 2007).

4.2. Quantification of different C functional groups in organic surface horizons

Carbon NEXAFS and ^{13}C NMR spectroscopy revealed similar depth trends of the contribution of different C functional groups to total C in the organic surface horizons of the Histic Leptosol *Fall*. However, consistently larger O-alkyl C contributions were reported by ^{13}C NMR compared to C NEXAFS spectroscopy (Fig. 4c). As evident from a comparison of the cross symbols in Fig. 7a–d with the respective panels (i–l) of Fig. 6, the differences are probably caused by systematic underestimation of O-alkyl C and overestimation of the other C functional

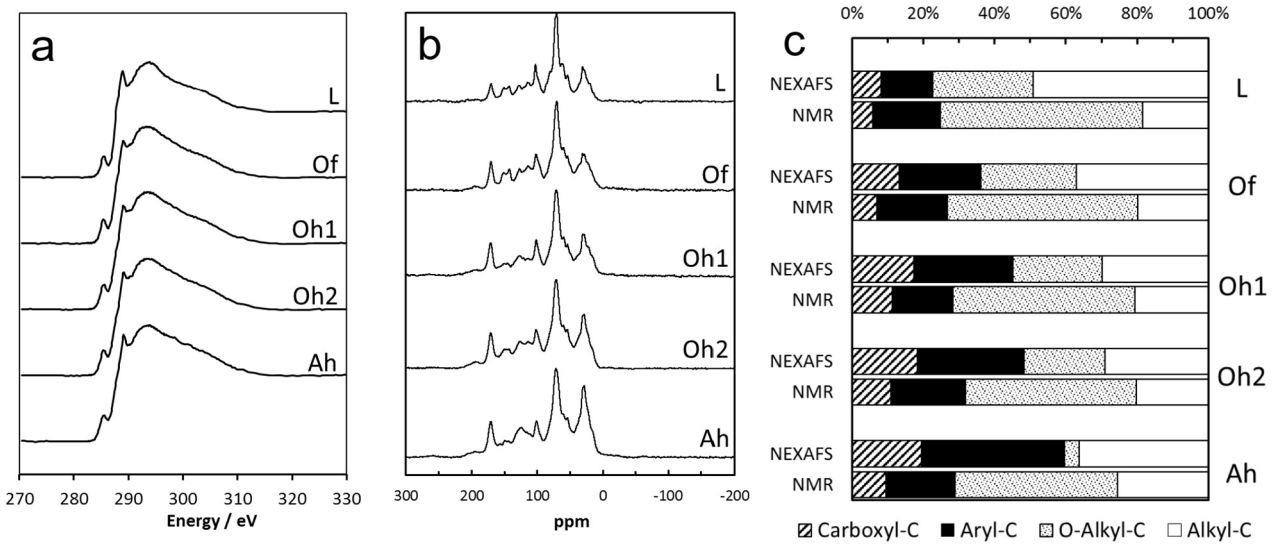

Fig. 4. (a) Normalized C NEXAFS, (b) CPMAS ^{13}C NMR spectra, (c) C speciation as quantified by NEXAFS and NMR spectroscopy for samples taken from different organic surface horizons of Histic Leptosol *Fall*.

groups with C NEXAFS compared to NMR spectroscopy. As noted above, the contribution of different C functional groups in our mixtures of major SOM sources as reported by CPMAS ^{13}C NMR spectroscopy agreed very well with their true contribution, whereas the results reported for the same mixtures by C NEXAFS spectroscopy were much less accurate and precise. This suggests that ^{13}C NMR spectroscopy also quantifies different C functional groups in organic surface horizons more correctly than C NEXAFS spectroscopy. With increasing depth and age of the organic surface horizons of *Fall* down to the Ah horizon, the alkyl C/O-alkyl C ratio as quantified by ^{13}C NMR spectroscopy increased

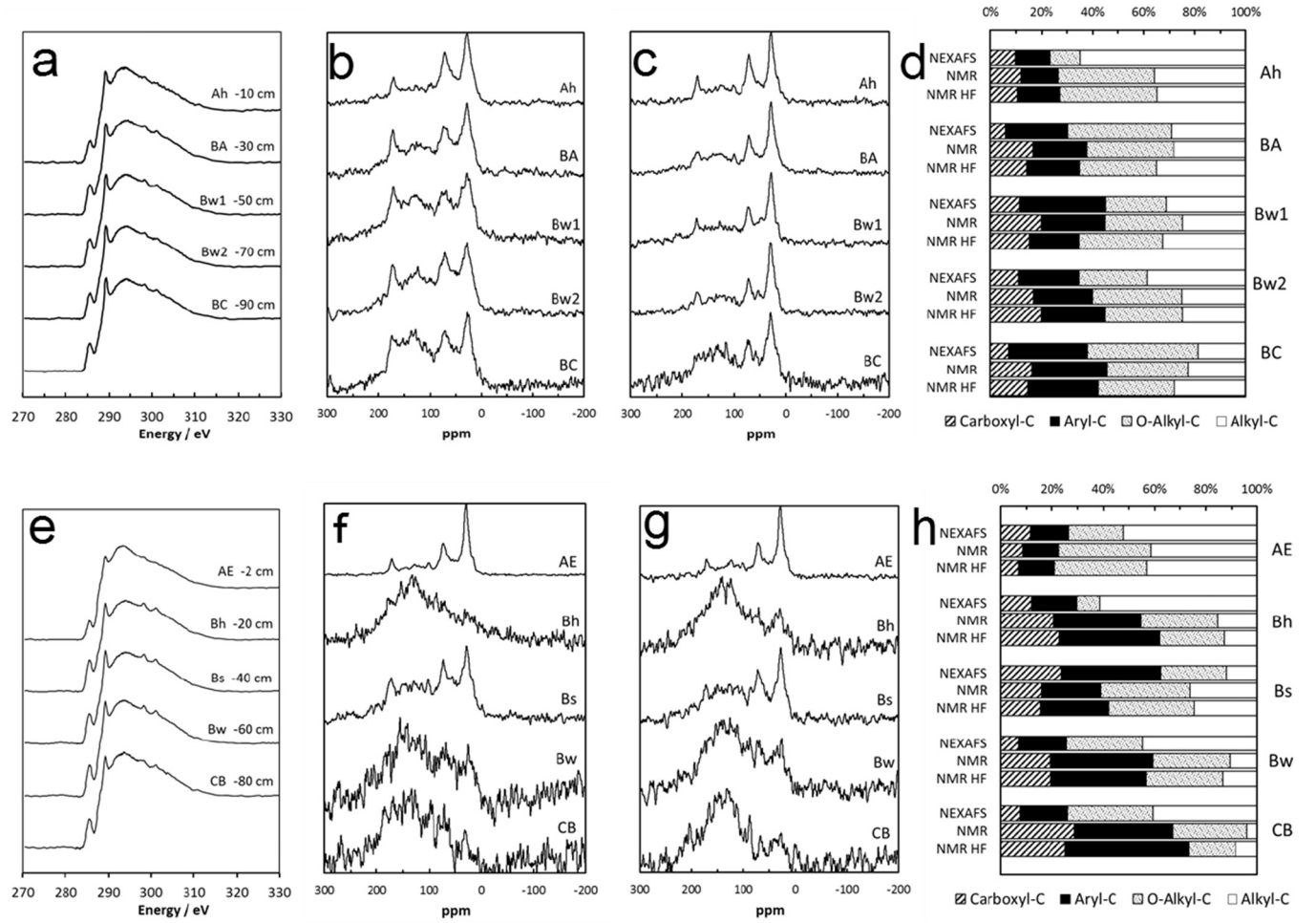

Fig. 5. (a,e) Normalized C NEXAFS, (b,f) CPMAS ^{13}C NMR spectra, (c,g) NMR spectra of HF-treated subsamples, and (d,h) C speciation as quantified by NEXAFS and NMR spectroscopy for samples from mineral soil horizons of (a–d) Cambisol *Mitterfels* and (e–h) Podzol *Luess*.

systematically (Table 5), indicating an increased SOM decomposition status with depth (Baldock and Preston, 1995; Baldock et al., 1997). Both the absolute percentages of different C species reported by CPMAS ^{13}C NMR spectroscopy in our study as well as the observed increase of the alkyl C/O-alkyl C ratio with depth agree well with results reported by Zech et al. (1985) for a similar Folic Histosol using the same technique. In contrast, the alkyl C/O-alkyl C ratios in the different organic surface horizons of *Fall* as quantified by C NEXAFS spectroscopy were considerably larger. This is probably due to the systematic underestimation of O-alkyl C by NEXAFS spectroscopy as described above. The absence of a depth trend for the alkyl C/O-alkyl C ratios in the organic surface horizons of *Fall* as reported by C NEXAFS spectroscopy (Table 5) contrasts with the results obtained by CPMAS ^{13}C NMR spectroscopy for the same samples. The discrepancy may be due to the low precision of C NEXAFS analysis, which masks any existing depth trend. Another explanation for the absent depth trend, however, may be the considerable recent SOM loss observed for the organic "Tangelhumus" surface layer of soil *Fall* caused by recently accelerated SOM mineralization due to climate warming (Prietzel et al., 2016). Increased SOM mineralization is likely associated with an increased mean SOM decomposition status (*i.e.* a larger alkyl C/O-alkyl C ratio) and probably most strongly affects the uppermost, least decomposed Of horizon, for which the largest alkyl C/O-alkyl C ratio of all O layers was reported by NEXAFS spectroscopy (Table 5). However, as stated above, different C functional groups in the *Fall* organic surface horizons, and thus also the alkyl C/O-alkyl C ratios, are likely reported more correctly by ^{13}C NMR than by C NEXAFS spectroscopy. Nevertheless, the discrepancy between the alkyl C/O-alkyl C depth trends reported by C NEXAFS and ^{13}C NMR spectroscopy remains to be fully explained.

Comparison of our NEXAFS data results with those obtained on forest soil organic surface layers in Switzerland and the USA (Schumacher et al., 2005; Keiluweit et al., 2012) showed similar percentages of aryl C (=aromatic+phenolic C; 10–30%). However, Keiluweit et al. (2012) reported markedly larger percentages of carboxyl C (35% of total C) compared to the percentages reported by Schumacher et al. (2005) and in our study (12% and 15–20%, respectively). Keiluweit et al. (2012) reported O-alkyl C contributions (about 25%) similar to those in our study (no data were presented for O-alkyl C by Schumacher et al., 2005). In contrast, the contribution of alkyl C in our study (30–35% of total C) was markedly larger than that (15%) reported by Keiluweit et al. (2012). The differences can be due to different spectra deconvolution procedures applied in both studies, but also due to markedly different environmental settings of the O layers in both studies. The "Tangelhumus" Oh layers in our study are formed under particular cool and moist climate and much older (^{14}C age up to >1000 years; Prietzel et al., 2013) than normal Oh horizons. In contrast, the O layers investigated by Keiluweit et al. (2012) had particular large abundances of ectomykorrhizal mats.

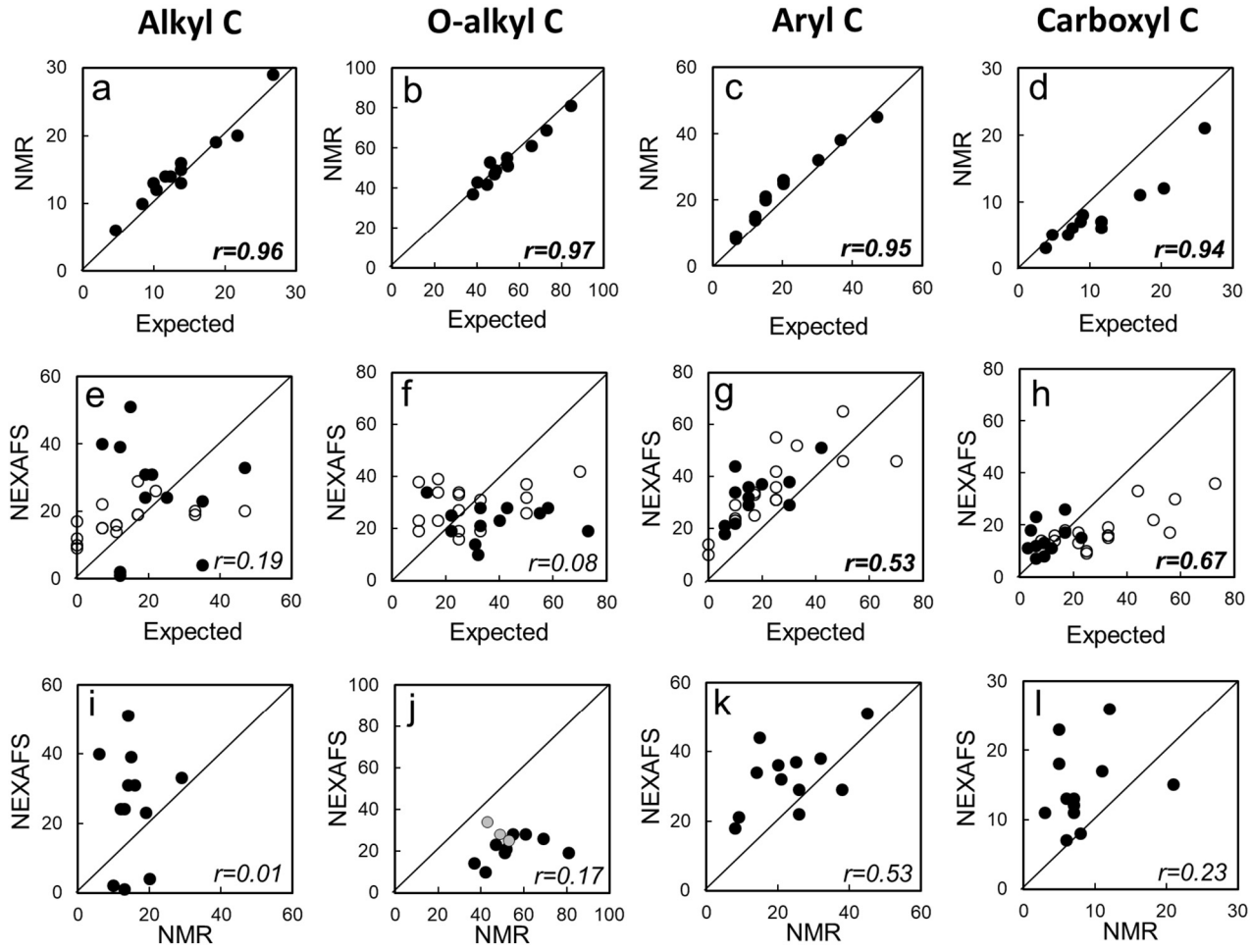

Fig. 6. Percentage of different C functional groups as reported by CPMAS ^{13}C NMR and C NEXAFS spectroscopy compared to true percentages of defined ternary and quaternary mixtures or organic compounds. Open circles: Set 1, consisting of graphite, L-glucose, Ca formate, and *L*-cysteine. Filled circles: Set 2, consisting of cellulose, lignin, and *L*-cysteine. O-alkyl C fraction quantitated by NMR spectroscopy, but not that quantitated by NEXAFS spectroscopy includes also N-alkyl C. Gray symbols in Fig. 6j represent samples 4, 8, and 12 with particularly large *L*-cysteine percentages. Statistically significant ($p > 0.01$) Pearson correlation coefficients *r* (lower right corner in each panel) are printed in bold numbers.

4.3. Quantification of different C functional groups in mineral topsoil horizons

In the A horizons of *Mitterfels* and *Lüss*, the percentages of carboxyl C (10% of total C) and of aryl C (15% of total C) as reported by C NEXAFS and ^{13}C NMR spectroscopy are fairly similar (Fig. 5d; Fig. 7c,d; filled symbols). Moreover, they agree well with the values reported by Schumacher et al. (2005) for soil colloids in Ah horizons of Swiss forest soils (mean percentages of carboxyl C and aryl C: 12% and 10%, respectively). This indicates that both methods reasonably well quantify these C functional groups in topsoil samples. However, this finding contrasts to results of Solomon et al. (2002, 2005) who reported markedly larger carboxyl C percentages (around 40% of total C) using C NEXAFS spectroscopy compared to (liquid-state) ^{13}C NMR and FTIR-ATR spectroscopy (10–20% of total C) for alkaline humic extracts from clay and silt fractions of tropical soil A horizon samples. The larger content of alkyl C compared to that of O-alkyl C in the A horizon of *Fall*, *Mitterfels*, and *Luess* as reported by C NEXAFS, but not by NMR spectroscopy in our study also is in contrast to Solomon et al. (2002, 2005). Similar to the *Fall* organic surface layers, we assume that also for the Ah horizons of our study, the OC speciation as reported by ^{13}C NMR spectroscopy probably is more correct than that reported by C NEXAFS spectroscopy.

4.4. Quantification of different C functional groups in mineral subsoil horizons

4.4.1. Cambisol Mitterfels

The C speciation patterns in the B and BC horizons of the Cambisol *Mitterfels* as reported by C NEXAFS and ^{13}C NMR spectroscopy are similar for all C functional groups except carboxyl C (Fig. 5d; Fig. 7a–d, open triangles). This indicates that both methods reasonably well quantify most OC functional groups, including alkyl C and O-alkyl C in the *Mitterfels* subsoil, which is characterized by OC concentrations >15 mg g^{-1} (Table 3) and OC/Fe$_d$ ratios >1.5 (Table 5). This is probably also true also for other subsoils with similar texture, OC, and Fe$_d$ contents. According to our results, SOM in the *Mitterfels* subsoil consists to a large portion (25–40% of SOC) of O-alkyl C, which is probably mainly bound in polysaccharides and associated with Fe, Al oxyhydroxides (Spielvogel et al., 2008). The second most important OC species in the *Mitterfels* subsoil is alkyl C (20–35% of SOC). Aryl C, probably mostly of root lignin origin (Spielvogel et al., 2008) is also present in significant amounts (25–30% of total C), whereas carboxyl C with 10–20% of OC is of minor relevance.

The negligible OC speciation change reported by NMR spectroscopy after HF treatment of a *Mitterfels* A horizon subsample compared to the untreated subsample (Fig. 7e–h, filled triangles) is in line with results obtained for humic topsoil horizons in earlier studies (Skjemstad et al., 1994; Schmidt et al., 1997; Spielvogel et al., 2008). In contrast, the alkyl C/O-alkyl C ratios reported by NMR spectroscopy on HF-treated subsamples taken from B and BC horizons of *Mitterfels* were consistently larger than the respective values obtained for untreated subsamples (Table 5). This increase is due to increased percentages of alkyl C and/or decreased percentages of O-alkyl C in the HF-treated compared the respective untreated *Mitterfels* B and BC horizon subsamples (Fig. 7e,f; open triangles). Moreover, treatment of B horizon samples with HF was associated with >80% mass loss and 40–60% OC loss (Table 5). Our findings support the statement of Spielvogel et al. (2008) based on studies on a nearby Cambisol derived from the same parent material, that microbial-derived polysaccharides (*i.e.* O-alkyl C) are preferentially associated to pedogenic Al and Fe minerals and thus preferentially mobilized by HF treatment (Eusterhues et al., 2003, 2005; Rumpel et al., 2002). Thus, in line with results from earlier studies (Dai and Johnson, 1999; Spielvogel et al., 2008; Sanderman et al., 2017), our results show that the C speciation of a HF-treated sesquioxide-rich soil sample which has lost most original OC by mobilization and dissolution during HF treatment, in many cases does not represent its C speciation prior to HF treatment.

4.4.2. Podzol Luess

For all mineral soil horizons of *Luess*, including those with OC concentrations <1 mg g^{-1} or OC/Fe$_d$ mass ratios <1, high-quality spectra with excellent signal-to-noise ratios were obtained by C NEXAFS spectroscopy (Fig. 5e). Synchrotron-based C NEXAFS spectroscopy (at least when performed at the powerful beamline U7B of NSLS with PEY detection) thus is a sensitive tool for the speciation of SOC in low-C subsoils. This is not the case for CPMAS ^{13}C NMR spectroscopy. Most NMR spectra acquired for the *Luess* B subsoil samples were very noisy and showed marked signal broadening (Fig. 5f), compromising a reliable spectra deconvolution and C speciation. This is in contrast to the high-quality CPMAS ^{13}C NMR spectra with excellent signal-to-noise-ratios obtained by for Podzol B horizons Spielvogel et al. (2008) using the same instrument and measurement protocol. However, that Podzol had considerably larger OC contents (11–27 mg g^{-1}) than *Luess*. Treatment of the *Luess* mineral soil samples with HF was associated with larger OC losses (70–90%) than total soil mass losses (50–80%; Table 5), resulting in decreased OC concentrations. It therefore did not lead to a satisfactory improvement of NMR spectrum quality (Fig. 5g), which would allow a reliable C speciation. The reason for the large sample OC concentration decrease by HF treatment of the *Luess* subsoil samples is that in the *Luess* subsoil the SOM is almost exclusively present as mixed Al/Fe oxyhydroxide-SOM co-precipitate forming coatings on quartz-sand grains (Werner et al., 2017b) which are released upon HF treatment. The OC speciation results obtained by deconvoluting the noisy CPMAS ^{13}C NMR spectra of the *Luess* B and CB horizon samples either without or after HF treatment (Fig. 5h) must therefore be interpreted with greatest caution and probably do not give a realistic picture of the real OC speciation in these horizons. In contrast, NEXAFS spectroscopy likely provides a fair estimate for the OC speciation of the *Luess* subsoil. This assumption bases on the facts that (i) the C speciation results obtained by C NEXAFS and ^{13}C NMR spectroscopy for the *Mitterfels* subsoil samples (open triangles in Fig. 7a–d) generally agreed well with each other, and (ii) the quality of the C NEXAFS spectra obtained for the *Luess* subsoil was excellent. According to the NEXAFS results (Fig. 5h), Bh and Bs illuvial horizons differ strongly from each other regarding their C speciation: Carboxyl C, aryl C, and O-alkyl C, are markedly enriched and alkyl C is depleted in the Bs horizon compared to the other mineral soil horizons of *Luess*, whereas the opposite is the case for the Bh. Consequently, the alkyl C/O-alkyl C ratios of both horizons differ markedly (Bh: 6.9; Bs: 0.5; Table 5). This finding indicates a gradual change of major SOM accumulation patterns in Podzol illuvial horizons with time. Initial SOM accumulation in these horizons is characterized by preferential sorption and co-precipitation of polysaccharides (Gu et al., 1994; Spielvogel et al., 2008) and aromatic moieties (Biber and Stumm, 1994; Kaiser and Zech, 2000) on/with pedogenic oxyhydroxides. With increasing OC saturation of the pedogenic oxyhydroxides in the upper part of the illuviation region (Bh horizon), more hydrophobic compounds rich in alkyl C get increasingly attached to previously retained, more hydrophilic SOM compounds (polysaccharides).

5. Conclusions

CPMAS ^{13}C NMR spectroscopy can accurately and precisely quantify different C functional groups in mixtures of important SOM source compounds, and probably also in SOM of organic surface and mineral topsoil horizons. In contrast to NMR spectroscopy, synchrotron-based C NEXAFS spectroscopy conducted at a powerful beamline can yield spectra with an excellent signal-to-noise ratio also for soil samples with low (<1 mg g^{-1}) OC content. It can directly and quickly semi-quantify different C functional groups in OC-poor subsoil samples, where CPMAS ^{13}C NMR spectroscopy faces serious problems with regard to spectrum

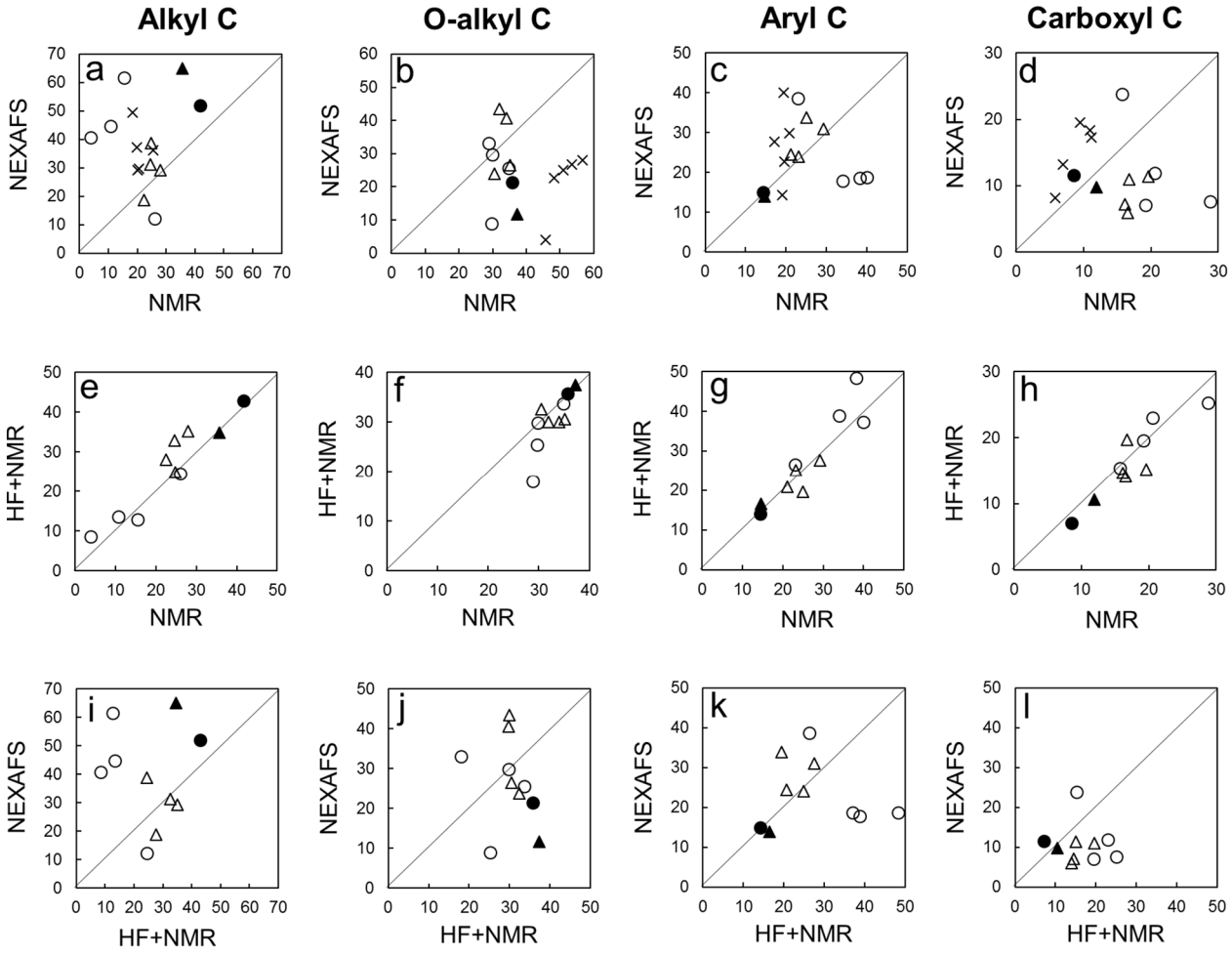

Fig. 7. Comparison of percentages of different C functional groups as reported by C NEXAFS spectroscopy, CPMAS ^{13}C NMR spectroscopy, and CPMAS ^{13}C NMR spectroscopy after subsample treatment with HF spectroscopy in organic surface horizons of Histosol Fall (crosses), as well as mineral soil horizons of Cambisol *Mitterfels* (triangles) and Podzol *Luess* (circles). Filled triangles and circles indicate A horizon samples of *Mitterfels* and *Luess*, respectively. O-alkyl C fraction quantitated by NMR spectroscopy, but not that quantitated by NEXAFS spectroscopy includes also N-alkyl C.

quality. This feature of C NEXAFS spectroscopy allows assessing the chemical composition of subsoil organic matter, which plays an important role as stable soil C pool but whose chemical composition is still poorly understood (Rumpel and Kögel-Knabner, 2011). C NEXAFS spectroscopy will become even more attractive for assessing the C speciation in C-poor subsoils when more sophisticated techniques of spectrum deconvolution (Heymann et al., 2011) and detailed spectra databases (Solomon et al., 2009) will likely improve the accuracy and precision of this method. It ultimately may permit a true quantitative rather than semi-quantitative C speciation in soils. Yet, the application of synchrotron-based techniques in soil science is subject to spatial and temporal accessibility constraints (large travel distance to synchrotron facilities with appropriate beamlines, limited beamtime). It therefore can only be one of several analytical tools in our soil scientific toolkit. In this context it is important to mention that – as well as other instrumental analytical methods – also NMR spectroscopy during recent years continuously has been improved regarding instrument capabilities, resolving power, and measurement techniques (Courtier-Murias et al., 2014; Johnson and Schmidt-Rohr, 2014; Simpson et al., 2012, 2018). Combination of various analytical SOC speciation methods, including NEXAFS, NMR, FT-IR (Fu and Quan, 2006; Heckman et al., 2011) and FTIR-ATR spectroscopy (Biber and Stumm, 1994; Solomon et al., 2005) will help to attain a better understanding of the speciation and turnover of organic matter in soils.

Acknowledgements

The study was funded by BLE Waldklimafonds (Grant 28WC406301). We want to thank Dr. E Windeisen (Wood Research München; Technical University of Munich) for providing us with specimens of cellulose and lignin. S. Hiesch and M. Weber assisted in CPMAS ^{13}C NMR spectra acquisition. Certain commercial names are presented in this manuscript for the purpose of illustration and do not constitute an endorsement by NIST.

References

Arshad, M.A., Ripmeester, J.A., Schnitzer, M., 1988. Attempts to improve solid state ^{13}C NMR spectra of whole mineral soils. Can. J. Soil Sci. 68, 593–602.

Baldock, J.A., Preston, C.M., 1995. Chemistry of carbon decomposition processes in forests as revealed by solid-state carbon-13 nuclear magnetic resonance. In: McFee, W.W., Kelly, J. M. (Eds.), Carbon Forms and Functions in Forest Soils. SSSA, Madison WI, pp. 89–118.

Baldock, J.A., Oades, J.M., Preston, C.M., Nelson, P.N., Skene, T.M., Golchin, A., Clarke, P., 1997. Assessing the extent of decomposition of natural organic materials using solid-state ^{13}C NMR spectroscopy. Aust. J. Soil Res. 35, 1061–1083.

Biber, M.V., Stumm, W., 1994. An in-situ ATR-FTIR study: the surface coordination of salicylic acid on aluminum and iron (III) oxides. Environ. Sci. Technol. 28, 763–768.

Chen, J., Gu, B., LeBoeuf, E.J., Pan, H., Dai, S., 2002. Spectroscopic characterization of the structural and functional properties of natural organic matter fractions. Chemosphere 48, 59–68.

Chen, C., Dynes, J.J., Wang, J., Karunakaran, C., Sparks, D.L., 2014a. Soft X-ray spectromicroscopy study of mineral-organic matter associations in pasture soil clay fractions. Environ. Sci. Technol. 48, 6678–6686.

Chen, C., Dynes, J.J., Wang, J., Sparks, D.L., 2014b. Properties of Fe-organic matter associations via coprecipitation versus adsorption. Environ. Sci. Technol. 48, 13751–13759.

Christl, I., Kretzschmar, R., 2007. C-1s NEXAFS spectroscopy reveals chemical fractionation of humic acid by cation-induced coagulation. Environ. Sci. Technol. 41, 1915–1920.

Cody, G.D., Ade, H., Wirick, S., Mitchell, G.D., Davis, A., 1998. Determination of chemical-structural changes in vitrinite accompanying luminescence alteration using C-NEXAFS analysis. Org. Geochem. 28, 441–455.

Cotrufo, M.F., Soong, J.L., Horton, A.J., Campbell, E.E., Haddix, M.L., Wall, D.H., Parton, W.J., 2015. Formation of soil organic matter via biochemical and physical pathways of litter mass loss. Nat. Geosci. 8, 776–779.

Courtier-Murias, D., Farooq, H., Longstaffe, J.G., Kelleher, B.P., Hart, K.M., Simpson, M.J., Simpson, A.J., 2014. Cross polarization-single pulse/magic angle spinning (CPSP/MAS): a robust technique for routine soil analysis by solid-state NMR. Geoderma 226–227, 405–414.

Dai, K.H., Johnson, C.E., 1999. Applicability of solid state 13CP/MAS NMR analysis in Spodosols: chemical removal of magnetic materials. Geoderma 93, 289–310.

Eusterhues, K., Rumpel, C., Kleber, M., Kögel-Knabner, I., 2003. Stabilisation of soil organic matter by interactions with minerals as revealed by mineral dissolution and oxidative degradation. Org. Geochem. 34, 1591–1600.

Eusterhues, K., Rumpel, C., Kögel-Knabner, I., 2005. Organomineral associations in sandy acid forest soils: importance of specific surface area, iron oxides and micropores. Eur. J. Soil Sci. 56, 753–763.

Fu, H., Quan, X., 2006. Complexes of fulvic acid on the surface of hematite, goethite, and akaganeite: FTIR observation. Chemosphere 63, 403–410.

Gu, B., Schmitt, J., Chen, Z., Liang, L., McCarthy, J.F., 1994. Adsorption and desorption of natural organic matter on iron oxide: mechanisms and models. Environ. Sci. Technol. 28, 38–46.

Heckman, K., Vazquez-Ortega, A., Gao, X., Chorover, J., Rasmussen, C., 2011. Changes in water extractable organic matter during incubation of forest floor material in the presence of quartz, goethite and gibbsite surfaces. Geochim. Cosmochim. Acta 75, 4295–4309.

Heymann, K., Lehmann, J., Solomon, D., Schmidt, M.W.I., Regier, T., 2011. C 1s K-edge near edge X-ray absorption fine structure (NEXAFS) spectroscopy for characterizing functional group chemistry of black carbon. Org. Geochem. 42, 1055–1064.

Johnson, R.L., Schmidt-Rohr, K., 2014. Quantitative solid-state ^{13}C NMR with signal enhancement by multiple cross polarization. J. Magn. Reson. 239, 44–49.

Jokic, A., Cutler, J.N., Ponomarenko, E., van der Kamp, G., Anderson, D.W., 2003. Organic carbon and sulfur compounds in wetland soils: insights on structure and transformation processes using K-edge XANES and NMR spectroscopy. Geochim. Cosmochim. Acta 67, 2585–2597.

Kaiser, K., Zech, W., 2000. Dissolved organic matter sorption by mineral constituents of subsoil clay fractions. J. Plant Nutr. Soil Sci. 163, 531–535.

Kaznacheyev, K., Osanna, A., Jacobsen, C., Plashkevych, O., Vahtras, O., Carravetta, H.V., Hitchcock, A.P., 2002. Innershell absorption spectroscopy of amino acids. J. Phys. Chem. A 106, 3153–3168.

Keiluweit, M., Bougoure, J.J., Zeglin, L.H., Myrold, D.D., Weber, P.K., Pett-Ridge, J., Kleber, M., Nico, P.S., 2012. Nano-scale investigation of the association of microbial nitrogen residues with iron (hydr)oxides in a forest soil O-horizon. Geochim. Cosmochim. Acta 95, 213–226.

Kinchesh, P., Powlson, D.S., Randall, E.W., 1995. ^{13}C NMR studies of organic matter in whole soils: I. Quantitation possibilities. Eur. J. Soil Sci. 46, 125–138.

Knicker, H., Lüdemann, H.D., 1995. N-15 and C-13 CPMAS and solution NMR studies of N-15 enriched plant material during 600 days of microbial degradation. Org. Geochem. 23, 329–341.

Kögel-Knabner, I., 1997. ^{13}C and ^{15}N NMR spectroscopy as a tool in soil organic matter studies. Geoderma 80, 243–270.

Lang, F., Krüger, J., Amelung, W., Willbold, S., Frossard, E., Bünemann, E.K., Bauhus, J., Nitschke, J.R., Kandeler, E., Marhan, S., Schulz, S., Bergkemper, F., Schloter, M., Luster, J., Guggisberg, F., Kaiser, K., Mikutta, R., Guggenberger, G., Polle, A., Pena, R., Prietzel, J., Rodionov, A., Talkner, U., Meesenburg, H., von Wilpert, K., Hölscher, A., Dietrich, H.P., Chmara, I., 2017. Soil phosphorus supply controls P nutrition strategies of beech forest ecosystems in Central Europe. Biogeochemistry 136, 5–29.

Lehmann, J., Solomon, D., 2010. Organic carbon chemistry in soils observed by synchrotron-based spectroscopy. In: Singh, B., Gräfe, M. (Eds.), Developments in Soil Science, Volume 34 Synchrotron-Based Techniques in Soils and Sediments. Elsevier Chapter 14.

Lehmann, J., Solomon, D., Kinyangi, J., Dathe, L., Wirick, S., Jacobsen, C., 2008. Spatial complexity of soil organic matter forms at nanometre scales. Nat. Geosci. 1, 238–242.

Lehmann, J., Solomon, D., Brandes, J., Fleckenstein, H., Jacobsen, C., Thieme, J., 2009. Synchrotron-based near-edge X-ray spectroscopy of natural organic matter in soils and sediments. In: Senesi, N., Xing, B., Huang, P.M. (Eds.), Biophysico-Chemical Processes Involving Natural Nonliving Organic Matter in Environmental Systems. John Wiley & Sons, Inc., Hoboken, NJ, USA.

Mehra, O.P., Jackson, M.L., 1960. Iron oxide removal from soils and clays by a dithionite-citrate system buffered with sodium bicarbonate. Clay Clay Miner. 7, 317–327.

Paul, E.A., Follett, R.F., Leavitt, S.W., Halvorson, A., Peterson, G.A., Lyon, D.J., 1997. Radiocarbon dating for determination of soil organic matter pool sizes and dynamics. Soil Sci. Soc. Am. J. 61, 1058–1067.

Peersen, O.B., Wu, X., Kustanovich, I., Smith, S.O., 1993. Variable amplitude cross-polarization MAS NMR. J. Magn. Reson. 104, 334–339.

Prietzel, J., Dechamps, N., Spielvogel, S., 2013. Analysis of non-cellulosic polysaccharides helps to reveal the history of thick organic surface layers on calcareous Alpine soils. Plant Soil 365, 93–114.

Prietzel, J., Zimmermann, L., Schubert, A., Christophel, D., 2016. Organic matter losses in German Alps forest soils since the 1970s most likely caused by warming. Nat. Geosci. 9, 543–548.

Ravel, B., Newville, M., 2005. ATHENA, ARTEMIS, HEPHAESTUS: data analysis for X-ray absorption spectroscopy using IFEFFIT. J. Synchrotron Radiat. 12, 537–541.

Rumpel, C., Kögel-Knabner, I., 2011. Deep soil organic matter – key but poorly understood component of terrestrial C cycle. Plant Soil 338, 143–158.

Rumpel, C., Kögel-Knabner, I., Bruhn, F., 2002. Vertical distribution, age, and chemical composition of organic carbon in two forest soils of different pedogenesis. Org. Geochem. 33, 1131–1142.

Sanderman, J., Farrell, M., Macreadie, P.I., Hayes, M., McGowan, J., Baldock, J., 2017. Is demineralization with dilute hydrofluoric acid a viable method for isolating mineral stabilized soil organic matter? Geoderma 304, 4–11.

Schaefer, J., Stejskal, E.O., 1976. Carbon-13 nuclear magnetic resonance of polymers spinning at the magic angle. J. Am. Chem. Soc. 98, 1031–1032.

Scheinost, A.C., Kretzschmar, R., Christl, I., Jacobsen, C., Ghabbour, Elham A., Davies, Geoffrey, 2001. Carbon group chemistry of humic and fulvic acid: a comparison of C-1s NEXAFS and ^{13}C NMR spectroscopies. Humic Substances: Structures, Models and Functions. Royal Society of Chemistry, Great Britain, pp. 39–47.

Schmidt, M.W.I., Knicker, H., Hatcher, P.G., Kögel-Knabner, I., 1997. Improvement of ^{13}C CPMAS NMR spectra of bulk soils, particle size fractions and organic material by treatment with 10% hydrofluoric acid. Eur. J. Soil Sci. 48, 319–328.

Schöning, I., Knicker, H., Kögel-Knabner, I., 2005. Intimate association between O/N-alkyl carbon and iron oxides in clay fractions of forest soils. Org. Geochem. 36, 378–1390.

Schumacher, M., Christl, I., Scheinost, A.C., Jacobsen, C., Kretzschmar, R., 2005. Chemical heterogeneity of organic soil colloids investigated by scanning transmission X-ray microscopy and C-1s NEXAFS microspectroscopy. Environ. Sci. Technol. 39, 9094–9100.

Schwertmann, U., 1964. Differenzierung der Eisenoxide des Bodens durch Extraktion mit Ammoniumoxalat-Lösung. Z. Pflanzenernähr. Bodenkd. 105, 194–202.

Simpson, A.J., Simpson, M.J., Soong, R., 2012. Nuclear magnetic resonance spectroscopy and its key role in environmental research. Environ. Sci. Technol. 46, 11488–11496.

Simpson, A.J., Simpson, M.J., Soong, R., 2018. Environmental nuclear magnetic resonance spectroscopy: an overview and a primer. Anal. Chem. 90, 628–639.

Skjemstad, J.O., Clarke, P., Taylor, J.A., Oades, J.M., Newman, R.H., 1994. The removal of organic materials from surface soils. A solid state ^{13}C CPMAS NMR study. Aust. J. Soil Res. 32, 1215–1229.

Skjemstad, J.O., Clarke, P., Golchin, A., Oades, J.M., 1997. Characterization of soil organic matter by solid-state ^{13}C NMR spectroscopy. In: Cadisch, G., Giller, K.E. (Eds.), Driven by Nature: Plant Litter Quality and Decomposition. CAB International, Wallingford, pp. 253–272.

Smernik, R.J., Oades, J.M., 2000. The use of spin counting for determining quantitation in solid state ^{13}C NMR spectra of natural organic matter 1. Model systems and the effects of paramagnetic impurities. Geoderma 96, 101–129.

Solomon, D., Fritzsche, F., Tekalign, M., Lehmann, J., Zech, W., 2002. Soil organic matter composition in the subhumid Ethiopian highlands as influenced by deforestation and agricultural management. Soil Sci. Soc. Am. J. 66, 68–82.

Solomon, D., Lehmann, J., Kinyangi, J., Liang, B., Schäfer, T., 2005. Carbon K-edge NEXAFS and FTIR-ATR spectroscopic investigation of organic carbon speciation in soils. Soil Sci. Soc. Am. J. 69, 107–119.

Solomon, D., Lehmann, J., Kinyangi, J., Liang, B., Heymann, K., Dathe, L., Hanley, K., Wirik, S., Jacobsen, C., 2009. Carbon (1s) NEXAFS spectroscopy of biogeochemically relevant reference organic compounds. Soil Sci. Soc. Am. J. 73, 1817–1830.

Spielvogel, S., Prietzel, J., Kögel-Knabner, I., 2008. Soil organic matter stabilization in acidic forest soils is preferential and soil type specific. Eur. J. Soil Sci. 59, 674–692.

Stöhr, J., 1996. NEXAFS spectroscopy. Springer Series in Surface Sciences Vol. 25. Springer, Berlin.

Wan, J., Tyliszczak, T., Tokunaga, T.K., 2007. Organic carbon distribution, speciation, and elemental correlations within soil microaggregates: applications of STXM and NEXAFS spectroscopy. Geochim. Cosmochim. Acta 71, 5439–5449.

Werner, F., de la Haye, T.R., Spielvogel, S., Prietzel, J., 2017a. Small-scale spatial distribution of phosphorus fractions in soils from silicate parent material with different degree of podzolization. Geoderma 302, 52–65.

Werner, F., Mueller, C.W., Thieme, J., Gianoncelli, A., Rivard, C., Höschen, C., Prietzel, J., 2017b. Micro-scale heterogeneity of soil phosphorus depends on soil substrate and depth. Nat. Sci. Rep. 7:3203. https://doi.org/10.1038/s41598-017-03537-8.

Wilson, M.A., 1987. N. M. R. Techniques and Applications in Geochemistry and Soil Chemistry. Pergamon Press, Toronto, Canada.

Zech, W., Kögel, I., Alt, H., 1985. CP-MAS-^{13}C-NMR-Spektren organischer Lagen einer Tangelrendzina. Z. Pflanzenernaehr. Bodenkd. 148, 481–488.